HHS Public Access

Author manuscript

Arch Environ Contam Toxicol. Author manuscript; available in PMC 2018 January 26.

Published in final edited form as:

Arch Environ Contam Toxicol. 2017 July ; 73(1): 63–75. doi:10.1007/s00244-017-0417-6.

Biomarkers of Aryl-hydrocarbon Receptor Activity in Gulf Killifish (*Fundulus grandis*) From Northern Gulf of Mexico Marshes Following the Deepwater Horizon Oil Spill

Benjamin Dubansky[1,4], **Charles D. Rice**[2], **Lester F. Barrois**[3], and **Fernando Galvez**[4]

[1]Department of Biological Sciences, Developmental Integrative Biology Cluster, University of North Texas, 225B Life Sciences Building, Denton, TX 76203, USA

[2]Department of Biological Sciences, Clemson University, 132 Long Hall, Clemson, SC 29634, USA

[3]L&A Industries, LLC, Belle Chasse, LA 70037, USA

[4]Department of Biological Sciences, Louisiana State University, 208 Life Sciences Building, Baton Rouge, LA 70803, USA

Abstract

Following the Deepwater Horizon oil spill, shorelines throughout the Barataria Basin of the northern Gulf of Mexico in Louisiana were heavily oiled for months with Macondo-252 oil, potentially impacting estuarine species. The Gulf killifish (*Fundulus grandis*) has been identified as a sentinel species for the study of site-specific effects of crude oil contamination on biological function. In November and December 2010, 4–5 months after the Macondo well was plugged and new oil was no longer spilling into the Gulf waters, Gulf killifish were collected across the Barataria Basin from 14 sites with varying degrees of oiling. Fish collected from oiled sites exhibited biological indications of exposure to oil, including increase in cytochrome P4501A (CYP1A) mRNA transcript and protein abundances in liver tissues. Immunohistochemistry revealed increases in gill, head kidney, and intestinal CYP1A protein at heavily oiled sites. Intestinal CYP1A protein was a sensitive indicator of exposure, indicating that intestinal tissue plays a key role in biotransformation of AHR ligands and that ingestion is a probable route of exposure, warranting additional consideration in future studies.

The Deepwater Horizon oil spill (DHOS) occurred on April 20, 2010, releasing more than 780 million liters of light crude oil into the Gulf of Mexico approximately 80 km from the Louisiana coast (McNutt et al. 2012; Turner et al. 2016). Unlike with other spills of heavier

Correspondence to: Benjamin Dubansky.

Author Contributions

The manuscript was written with contributions by all of the authors. All authors have given approval to the final version of the manuscript. B. D. collected all samples.

Compliance with Ethical Standards

Conflict of interest

The authors declare no conflict of interest.

Electronic supplementary material The online version of this article (doi:10.1007/s00244-017-0417-6) contains supplementary material, which is available to authorized users.

crude oils, the Macondo oil from the DHOS underwent a more rapid weathering prior to its landfall (Liu et al. 2012). Shoreline Cleanup and Assessment Technique (SCAT) operations by the federal, state, local, and British Petroleum (BP) representatives documented that more than 2113 km of Gulf of Mexico shoreline were oiled. Approximately 1364 km occurred in the northern Gulf of Mexico shorelines of Southern Louisiana (Nixon et al. 2016). One of the most affected areas in Louisiana was the Barataria Basin, which covers approximately 5720 km^2 of estuarine marsh and open water (Kokaly et al. 2013). However, even in the most heavily oiled regions, oil coverage was heterogeneous in time and space. Indeed, chemical analysis of affected shoreline revealed that Macondo oil and its chemical constituents varied by as much as tenfold in concentration over a distance of a few meters (Turner et al. 2014). This heterogeneity in field oiling made it difficult to assess exposure conditions to biota in affected areas. Furthermore, although the concentrations of oil-derived toxicants in water often were low, many components of crude oil, such as benzo-[*a*]-pyrene (BaP), naphthalene, chrysene, and fluoranthene, remained highly elevated in sediment well after much of the visible oiling was gone (Crowe et al. 2014; Dubansky et al. 2013; Pilcher et al. 2014; Tuvikene 1995).

Several PAHs in crude oil, including many of its most persistent derivatives, exert their toxicity through the aryl-hydrocarbon receptor (AHR), a ligand-activated transcription factor (Lindsey and Papoutsakis 2012; Stevens et al. 2009). PAHs bind to the AHR in the cytosol, which becomes chaperoned to the nucleus, evoking the induction of xenobiotic metabolizing enzymes, including phase I, II, and III components of metabolism, and transporters that promote the excretion of xenobiotics (Abel and Haarmann-Stemmann 2010). As such, exposure to AHR-active PAHs in crude oil is often assessed by measuring AHR pathway-related genes and gene products (Celander 2011; Reinecke and Segner 1998; Spies et al. 1996; Woodin et al. 1997).

Cytochrome P4501A (CYP1A) is among a family of xenobiotic metabolism enzymes within the AHR pathway that biotransform PAHs during metabolism to reactive intermediates, thus activating these contaminants to exert their toxic effects (Hogan et al. 2010; Nakayama et al. 2008). Hepatic CYP1A is the most common endpoint in quantifying exposure to PAHs in both laboratory and field studies (Dubansky et al. 2013; van der Oost et al. 2003). However, although the liver is considered the primary site of xenobiotic metabolism, AHR activity occurs in several extrahepatic tissues, including endothelial, and mesonephric and pronephric tissues, indicating that xenobiotic metabolism occurs throughout the body, but also in epithelia as part of its barrier function (Carlson et al. 2004a, b; Dubansky et al. 2013; Pilcher et al. 2014; Reynaud and Deschaux 2006; Rice 2001; Sarasquete and Segner 2000; Van Veld et al. 1988, 1990). Noting the high surface to volume ratio in the gills and intestine, the contribution to xenobiotic metabolism in these tissues is likely significant.

Exposure to PAHs dissolved in the water column can occur in the gills, which are in direct contact with the water, and through the intestine due to the ingestion of PAH-laden food, or from drinking water as part of osmoregulation in seawater fishes (McCormick 2001; Van Veld et al. 1988, 1990). Accordingly, the gill and intestine represent major routes of PAH exposure, but also have the capacity to metabolize PAHs before systemic transport (James et al. 2001; Levine and Oris 1999). The pronephric kidney (head kidney) is a major lymphoid

organ in teleostean fish, and PAHs are immunotoxic to fish in both field and laboratory studies (Nakayama et al. 2008; Rice 2001). It also is thought that metabolic activation of PAHs, as they cross the epithelial barriers, is part of the overall immunotoxicity of these compounds (Carlson et al. 2004a, b; Hogan et al. 2010; Reynaud and Deschaux 2006; Rice 2001). Considering the functional significance of these tissues, differential biological responses to PAHs can indicate routes of exposure and the potential for biological effect. However, despite the sensitivity of organismal and tissue-level responses to PAHs, it is difficult to link exposure to PAHs to chemical composition of environmental samples, in situ. As such, biomarkers of oil exposure present a useful tool to assess the presence of toxicants and the link to extent of exposure or effects in local biota.

Following the DHOS, several studies have demonstrated activation of the AHR pathway in organisms exposed to DHOS oil (Atlas and Hazen 2011; Crowe et al. 2014; Dubansky et al. 2013; Kokaly et al. 2013; Pilcher et al. 2014; Silliman et al. 2012; Whitehead et al. 2012). However, these studies have either involved laboratory exposures or have studied only a small number of oiled field sites. Certainly, due to the large area of oiled shoreline in the Barataria Basin and the potential for long-term impacts, the use of a biomarker approach to assess the extent of DHOS would be useful. However, estimating oiling in the field is difficult given the heterogeneity of physiochemical characteristics in this estuary in time and space. During remediation efforts, chemical analysis was largely conducted on individual sediment samples (grab samples), which may belie the extent of toxicity at locations, because grab samples depict the composition at a single discrete location and at a single point in time. Considering the varying coverage of crude oil in the Barataria Basin and the different home ranges of organisms of interest, composite sampling of sediments are likely more helpful at estimating the general toxicity at a study location (Dubansky et al. 2013). Furthermore, water chemistry also fluctuates as tides and currents heavily influence the physiochemical characteristics of the water, so the use of passive sampling devices is prudent to provide a cumulative estimates of water quality, *in lieu* of grab samples that cannot account for the ongoing fluctuations in water chemistry (Carls et al. 2004). Timing of sampling, combining diverse sampling methodologies (i.e. grab, composite, passive), site-specific effects (i.e. hydrology, weather events, land barriers, etc.), and other considerations can severely limit the direct comparison of such data between studies. Importantly, although the abundance of visible oil following the DHOS was estimated through SCAT surveys, it is still unclear whether the operational categories of oiling used in SCAT surveys correlated with the biological efficacy of oiling in the field (Turner et al. 2014).

A field study was conducted to test the hypotheses that: (1) AHR activity is greater in fish that live near oiled sites, and (2) this biological response correlates with the degree of visible oiling reported by SCAT surveys. To test these hypotheses, Gulf killifish, *Fundulus grandis*, were collected from differentially oiled sites and were sampled to compare biological response using markers of AHR activity.

Materials and Methods

Collection of Adult Fish

Gulf killifish were collected from 14 locations. Sampling locations were based on SCAT data (http://gomex.erma.noaa.gov) that assessed the degree of oiling at these locations during remediation efforts following the DHOS. Detailed SCAT assessment of the Barataria Basin partitioned shoreline oiling into discrete categories based on extensive visual observations of SCAT team members. Reference (unoiled) and oiled sites were chosen based on available SCAT oiling survey data at the time of sampling, between October and December 2010 (Table 1).

Adult fish were collected using wire minnow traps deployed along the shoreline approximately every 5 m, within 3 m of the shoreline. Twenty-five fish were collected and removed from the traps at each site and sampled in situ following measurement of length and mass (average length 77.89 mm ± 12.98 SE; mass 6.75 g ± 1.12 SE). Livers from eight of the fish collected at each site were dissected and placed in RNAlater (Ambion®), were kept on ice for transport, and then were stored at −20 °C until mRNA analysis. Livers from 12 more fish per site were flash frozen in liquid nitrogen and stored at −80 °C until use for relative quantification of CYP1A protein, as described below. The remains of five fish per site were fixed whole in Z-fix® buffered zinc formalin (Ameresco®), after opening the peritoneal cavity to allow penetration of fixative for histological processing of tissues as described below. All fish were handled according to institutional animal care and use committee (IACUC) protocol to minimize stress, pain, and discomfort.

Fish Tissue Processing

mRNA Levels of Candidate Genes—Two mRNA transcripts were measured in liver homogenates from fish collected from each location ($N = 7–8$). CYP1A mRNA was measured as an indicator of AHR induction, and aryl-hydrocarbon receptor repressor (AHRR) mRNA was measured as an indicator of regulation of AHR signaling. Total RNA was isolated using the TRIzol method according to the directions provided by the manufacturer (TRIzol®, Invitrogen), and quality was verified using microcapillary gel electrophoresis (Experion®, Bio-Rad Laboratories). cDNA synthesis was completed using the SuperScript® III First-Strand Synthesis SuperMix for qRT-PCR (Invitrogen) to generate cDNA for each sample. Specific relative gene expression was analyzed by quantitative real-time PCR with a Biorad iC5 detection system using specific target primer sets (Table 2) and RT^2 SYBR green/fluorescein master mix. The relative quantity of these mRNA transcripts was expressed as fold-changes in gene expression compared with 18S expression, measured using the Pfaffl method (Pfaffl 2001).

ELISA Detection of CYP1 Protein Expression—Relative CYP1A protein content in the livers ($N = 12$) was quantified using enzyme-linked immunosorbent assays (ELISA) using monoclonal antibody (mAb) C10-7 (Rice et al. 1998). Livers were thawed on ice, weighed, and individually homogenized in ice-cold homogenization buffer (0.25 M sucrose, 0.05 M Tris-base, 1 mM EDTA, 1 mM DTT, 0.1 mM PMSF). Homogenates were centrifuged at 10,000 g at 4 °C for 20 min to separate the nuclear fractions from the

cytosolic fractions. The upper layer of fat from each tube was aspirated and the supernatants, which contained the cytosolic components of the cells, transferred to new tubes and centrifuged at 100,000×*g* for 70 min. The resulting supernatants from the second spin were removed and stored for future use and the pellets containing the microsomal fraction were resuspended in a 5% glycerol resuspension buffer (0.25 M sucrose, 0.01 M HEPES, 0.1 mM EDTA, 0.1 mM DTT, 0.2 mM PMSF), aliquoted, and stored at −80 °C until use.

Ten additional fish were collected from an un-oiled location at the Louisiana Universities Marine Consortium (LUMCON) facility in Cocodrie, LA, as above, and were subsequently injected with benzo-[a]-pyrene (BaP), a potent inducer of the AHR pathway, for use as a positive control in ELISA assays for CYP1A. These fish were acclimated for 1 month to laboratory conditions, were given intraperitoneal injections of BaP (50 mg/kg) to induce AHR activity, and then were sacrificed at 48 h after injection. Livers were collected and microsomal fractions were prepared (as above), then pooled and homogenized. Homogenized liver microsomal fractions from positive control fish served as both a positive control and to control for plate-to-plate variation in optical density and to control for potential interassay differences.

Microsomal protein content was determined using the bicinchoninic acid protein assay (Thermo Scientific, Pierce). Microsome samples from each liver were diluted with phosphate-buffered saline (PBS) to a final protein concentration of 50 μg, and dispensed in triplicate to poly-L-lysine coated 96-well plates. Plates were incubated overnight at 4 °C, washed three times in PBS with 0.05% Tween-20, and blocked with PBS with 3% fetal bovine serum to prevent nonspecific binding. Plates were washed again before incubating with 100 μl mAb C10-7 (5 μg/ml) for 1.5 h at room temperature. Plates were then washed again and incubated with 100 μl of alkaline phosphatase (AP) conjugated goat-anti mouse immunoglobulin (IgG) (1:1500) in PBS (Sigma-Aldrich) for 1 h. Plates were washed again, and AP activity was quantified using p-nitrophenol phosphate (1 mg/ml) in AP buffer (100 mM NaCl, 5 mM $MgCl_2$, 100 mM Tris–HCL, pH 9.5). The optical density of each well was measured at 405 nm for 30 min. Each plate contained the same BaP-induced sample as an internal control.

Immunohistochemistry of Gill, Head Kidney, and Intestine—Whole fish (N = 4–5) were dissected to remove gills, head kidneys, and intestines from preserved fish. Tissues were dehydrated by a graded series of ethanol washes before clearing in Histochoice® Clearing Agent (Ameresco), before embedding in Paraplast X-tra® (Fisher Scientific) embedding media. Embedded tissues were cut to a thickness of 4–5 μm using a Microm HM 330 microtome (Heidelburg), and sections adhered to poly-L-lysine-coated glass microscope slides and stored at room temperature until staining. Slides were rehydrated and processed for immunohistochemical localization of CYP1A using monoclonal antibody (mAb), C10-7, according to Dubansky et al. (2013). Briefly, the Vectastain ABC immunoperoxidase system combined with NovaRed® (Vector Laboratories) was used to probe mAb C10-7 to indicate CYP1A protein as a deep red color, before counterstaining with Hematoxylin QS® (Vector Laboratories). All tissues, sections, and slides were processed identically, including incubation times with antibodies and hematoxylin staining.

Antibody-probed slides were subjectively scored based on the localization and intensity of immunoreactivity with CYP1A protein (red color) in cells that characteristically express CYP1A upon exposure to AHR-activating ligands, in the gill, head kidney, and intestine (Sarasquete and Segner 2000). Each tissue was observed and scored according to localization and abundance of staining for CYP1A. Each tissue was given a score based on the sum of two categories. Categories for the gill were (1) pillar cell staining and (2) all other cells (i.e. epithelial cells, mucus cells, vascular endothelial cells). Categories for the head kidney were (1) tubule cells and (2) vascular endothelial cells. Categories for the intestine were (1) cells of the mucosal layer and (2) vascular endothelial cells. Each category was ranked 0–3, based on CYP1A staining intensity, such that the combined maximum score of each tissue was 6 (Table 3). Gills were assessed for the presence or absence of CYP1A staining to: (a) pillar cell, and (b) other gill cells, including epithelial cells, mucus cells, and vascular endothelial cells (Fig. 1a). Head kidneys were monitored for the absence or presence of CYP1A staining to: (a) tubules, and (b) vascular endothelia (Fig. 1b). Intestines were scored similarly for CYP1A staining to: (a) mucosal layer cells and (b) submucosal cells for vascular endothelial cell staining characteristics (Fig. 1c).

SCAT Value Comparisons

For comparison between visible oiling and CYP1A staining intensity, numerical values were assigned to SCAT visible oiling color designations for heavy oiling (red = 6), moderate oiling (orange = 5), light oiling (yellow = 4), very light oiling (green = 3), tar balls (grey = 2), and no visible oiling (blue = 1; Table 4). SCAT values obtained from within 100 m of each sampling location were averaged based on the presumed limited home range of *F. grandis* (Fodrie et al. 2014b). Correlation between visible oiling and IHC scoring, mRNA, and ELISA results were determined using Spearman's Rank Order Correlation. Averaged values from all reference site fish versus all oiled site fish were compared using *t* tests. All statistical testing were completed using SigmaPlot 12.0 (Systat Software, Inc).

Imaging

Microscopy was performed on a Nikon Eclipse 80i microscope using Nikon DSFi1 camera and NIS-Elements BR 3.10 software. Images were balanced globally in Photoshop CS6® (Adobe) using the curves tool or the levels function for white balance. No additional adjustments were made locally to any images or portions thereof.

Results and Discussion

Field Oiling

Following the DHOS, SCAT surveys were conducted to assess relative oiling across the northern Gulf of Mexico coast. In the current study, SCAT data, obtained between October and December 2010 at 14 locations in Barataria Bay, Louisiana, were used to characterize the degree of visible oiling at Gulf killifish field collection sites. These SCAT survey data were reasonably consistent with our own anecdotal assessments of oiling at the time of fish collection (*data not shown*). Unlike what was observed in earlier field sampling of Barataria Bay marsh in June 2010, when oil was present on the surface water, marsh vegetation, detrital layer, and sediments (Dubansky et al. 2013; Whitehead et al. 2012), most of the oil

was portioned to the sediment by October–December 2010. In fact, as early as August 2010, water contained negligible levels of petroleum derivatives even at heavily oiled marsh sites (Dubansky et al. 2013; Whitehead et al. 2012). In contrast, sediments of heavily oiled sites contained very high concentrations of PAHs and were acutely toxic to developing Gulf killifish embryos for at least 18 months after the DHOS (Dubansky et al. 2013). Although SCAT data of visible oiling are semiquantitative and lack analytical chemistry, they may provide an indication of locations that were contaminated by oil.

CYP1A Protein Levels and CYP1A and AHRR mRNA Levels—Indicators of CYP1A induction were strongly associated with oiled sites. Average AHR-mediated CYP1A protein and CYP1A mRNA transcript levels were significantly increased in fish from oiled sites compared to unoiled sites ($P < 0.05$, t test; Figs. 2d–e). Despite the association of elevated CYP1A with higher SCAT values, the correlations were not significant, most likely because of the inadequate statistical power with the small number of sampling sites (CYP1A protein $R = 0.424$, $P = 0.125$, Spearman's rank order correlation, $df = 12$; CYP1A mRNA $R = 0.255$, $P = 0.373$, Spearman's rank order correlation, $df = 12$). Liver AHRR mRNA transcript abundance also was not correlated with the degree of oiling at each site ($R = -0.009$, $P = 0.964$, Spearman's rank order correlation, $df = 13$), and the average expression of AHRR mRNA transcripts at all oiled sites combined was not different compared with reference locations ($P = 0.430$, t test; Figs. 2c, f). Variation between CYP1A protein and mRNA, and AHRR mRNA in field-caught fish may be indicative of exposure to a varying distribution and abundance of oil mobilized from unseen accumulations beneath the surface, which may be present at each location where oiled shoreline had eroded at increased rates (Turner et al. 2016). This also suggests that visible oiling designations assigned during SCAT surveys are not descriptive of the chemical character of the surrounding aquatic environment.

An analysis between these data and data from ongoing and future remediation efforts will be helpful to describe the relationship between biological indicators of exposure and chemical characteristics in the environment. Although much of the Barataria Basin was considered heavily oiled, the distribution of oil in sediments has been described as patchy (Mendelssohn et al. 2012). As a result, aquatic organisms likely encountered varying concentrations of toxicants from oil as they traveled across their home ranges (Fodrie et al. 2014b). This heterogeneous distribution of oil in the Barataria Basin could account for some of the variability in biological response seen between sites. Furthermore, the lack of correlation between CYP1A protein and mRNA levels in the liver, and degree of visible oiling, suggests that SCAT data can only be considered a general predictor of exposure of marsh fish to Macondo oil. These data also are suggestive that in dynamic field studies where environmental variables might confound results, using markers of hepatic AHR activity alone are not entirely descriptive of the degree of site-specific PAH exposure. CYP1A mRNA was less correlated to indicators of visible oiling than CYP1A protein, and AHRR mRNA was not significantly correlated to oiling. This may be illustrative of the delay in timing and duration of molecular events between AHR activation, mRNA production, and subsequent translation to the functional protein, and perhaps discrepancy between translational activity and protein turnover rate. We note that although average AHR activity

was greater in fish from sites that had visible oiling, the biological response did not correlate to the degree of visible oiling at the sites.

IHC Localization of CYP1A in Gill, Head Kidney, and Intestine

Average subjective scoring of gill tissues for all fish gills collected from oiled sites were higher than the average gill score from reference site fish ($P = 0.002$, t test; Fig. 3d and Online Resource 1). Despite this, there was no significant correlation between IHC scoring in the gill and visible oiling between sites ($R = 0.424$, 0.125, Spearman's rank order correlation, $df = 12$). CYP1A protein was seen mostly in the pillar cells in the secondary lamellae of gills from fish collected at sites where SCAT data reported visible oiling. CYP1A protein expression in pillar cells is an indication of AHR-mediated activity and suggestive of an increase in exposure to PAH-derived ligands at these sites, as illustrated in Fig. 1a (Online Resource 1) (Levine and Oris 1999; Sarasquete and Segner 2000). Few fish showed signs of CYP1A expression in the epithelial cells of the gills, or elsewhere along the gill filament, which likely indicates low levels of AHR ligands in the water column at these sites. Gill tissues from Site O7 (St. Mary's Point) had the highest CYP1A expression scores, which likely indicate water-borne exposure to PAHs at this heavily oiled site (Levine and Oris 1999; VanVeld et al. 1997). No other sites had notable CYP1A protein expression in the gills other than Site R4, in northwest Bay Sansbois. At this reference site, there was increased CYP1A protein expression in the intestine and head kidneys (see below). Crude oil could be elevated in sediments below the water surface, in the absence of elevated PAH values in the water column, resulting in an increased exposure response (Dubansky et al. 2013). However, this scenario is not likely, because this site was more than 1 km from the nearest oiled shoreline and was protected from heavily oiled areas in Bay Batiste by Bayou Du Lac. Because R4 is situated in a narrow pass that serves as a bottleneck for travel from Bay Sansbois northwest to Myrtle Grove and Lake Hermitage, it is more likely that PAHs from boat traffic caused the increased immunoreactivity to CYP1A, rather than oil from the DHOS.

Head kidney tissues from designated oiled sites had a marked increase in CYP1A protein in the tubular epithelium and an increase in the staining of the vascular endothelial cells, as illustrated in Fig. 1b (Online Resource 1). Average scores for oiled sites were significantly elevated compared to reference sites ($P = 0.002$, t test; Fig. 3e), even though there was no significant correlation between the average CYP1A scoring of the tissue and average visible oiling at each site ($R = 0.516$, $P = 0.056$, Spearman's rank order correlation, $df = 12$; Fig. 3b), likely due to the low number of samples and small number of sites. Some reference site fish showed mild to moderate staining of CYP1A, albeit to a much lesser extent than the fish from oiled sites. Moderate basal CYP1A protein was common in the proximal tubules of the head kidney in fish from both oiled and reference sites, although this was highly variable between fish (data not shown). This is consistent with the observation that CYP1A is constitutively expressed in these tubular epithelial cells in field-caught fish from both reference and oiled locations (Dubansky et al. 2013). Conversely, CYP1A protein was rarely observed in the distal tubules of the head kidney, except at Site O7, the most heavily oiled location at St. Mary's Point, and at Site O9 in northeast Bay Batiste, where oil was reported as moderate. Similar to the gills, Site R4 in northwest Bay Sansbois also had increased

expression of CYP1A in the head kidneys. Indication of CYP1A expression in the head kidneys could indicate that increased exposure levels at these sites resulted in systemic transport of PAHs, because AHR ligands must first pass the barrier of the epithelium to access systemic transport to these internal tissues (see below).

Increased CYP1A protein was found in vascular endothelial cells of the head kidney to be differentially expressed between oiled and reference sites and is largely responsible for the overall increase in CYP1A protein expression in the head kidneys when comparing scores from all oiled versus all reference sites (Fig. 3e). Increased CYP1A expression in vascular endothelia is a hallmark of exposure to AHR-binding PAHs, making it an important diagnostic indicator of exposure (Sarasquete and Segner 2000). This increased CYP1A expression in the head kidneys could be indicative of immunotoxicity, because a number PAHs found in crude oil are known to be immunotoxic to vertebrates (Carlson et al. 2004b; Reynaud and Deschaux 2006). Furthermore, the increase in CYP1A expression in the vascular endothelia of the head kidney in fish from oiled sites is a clear indication of systemic transport of AHR-activating ligands, which have escaped first pass metabolism of the intestine and gills.

Intestinal tissue appeared to be the most obvious histological indicator of exposure to PAHs (Figs. 3c and Online Resource 1). Although CYP1A is induced in multiple tissues when in proximity to contaminated sediment, expression is greatest in the intestine, compared to other tissues when the route of exposure is through oiled food (Woodin et al. 1997). However, the average scores for oiled sites were not significantly elevated compared with intestines from reference sites ($P = 0.055$, t test; Fig. 3f and Online Resource 1). Furthermore, CYP1A protein levels in the mucosal cells of the intestine did not correlate to the degree of oiling determined by SCAT surveys at the time of sampling ($R = 0.516$, $P = 0.56$, Spearman's rank order correlation, $df = 12$; Fig. 3c). The absence of a statistically significant correlation and difference between conditions most likely reflects inadequate statistical power stemming from the limited number of sites evaluated and the small sample size ($N = 4–5$). Visibly, intestinal tissue sampled from oiled locations had markedly more pervasive and darker staining in the mucosal layer compared with fish sampled from reference sites (obvious in Fig. 1 and Online Resource 1). From this information, combined with the relatively low levels of CYP1A protein found in the gills compared with the intestine and head kidney, there is evidence that the uptake of PAHs was largely occurring from ingestion at the time of sampling.

First pass metabolism of xenobiotics can occur as they cross the intestinal epithelium, thus reducing the systemic load of PAHs to the liver, head kidneys, and other internal organs (James et al. 2001; Woodin et al. 1997). Metabolism of AHR-binding PAHs as they cross the epithelia likely influences the expression of AHR-related biomarkers in internal organs, such as the liver and head kidney, and to some degree the gill tissue, if exposure is dietary. The intestinal epithelial is optimized for increased surface area for transport and biotransformation of metabolites before entering the blood. If the contaminant load is eliminated or reduced by the metabolic capacity of the intestinal epithelia prior to circulatory transport, it is conceivable that the effective molecular response from the epithelia will be reflected in a reduced response in systemic tissues such as the liver or head kidney. If this is

the case, it would not be surprising if a reduced biomarker response is seen in, for example the liver, despite exposure to environmental PAHs through the diet. This could account for a lack of statistically significant correlations between liver tissues from field studies and sites that are differentially contaminated or otherwise have variability in contaminant levels over time and space.

The route of exposure to PAHs from crude oil also could account for the variability of CYP1A protein and mRNA transcript abundance of both CYP1A and AHRR observed within and between sites, where bioavailability of the toxicants can also be variable. Because highly increased CYP1A expression in the gills was found only in the most heavily oiled site (Site O7), one other oiled site (O9), and one reference site with heavy boat traffic (Site R4), it can be inferred that those fish were likely exposed to PAHs through the water. In contrast, fish at less oiled sites were likely exposed to PAHs through ingestion of food associated with oiled sediment, based on a higher relative expression in the intestine compared to the gills. Further study is warranted to understand the dynamics of this relationship of intestinal exposure to PAHs to determine if there is a difference in anterior regions of the intestine where food is absorbed compared with the posterior portions, which are more involved in water absorption in marine fish. Laboratory-based studies can be conducted to pinpoint the basis of this assumption, although these data support the hypothesis that fish at oiled sites (with the exception of O7 and O9) were primarily exposed to AHR-active ligands through the intestine at the time of sampling. It follows that sustained exposure from crude oil will likely occur through ingestion of benthic organisms living in oil-laden sediments (Woodin et al. 1997), and inadvertent consumption of toxicants in oiled sediments, in addition to direct contact with contaminants in the water column (Van Veld et al. 1997). The associations between AHR pathway activity and the presence and abundance of crude oil may provide benchmark data for comparison of ongoing remediation efforts and for future responses to anthropogenic alteration of habitat, which should include fine-scale indices of biological activity in intestinal, gill, and head kidney tissues.

It is important to note that Gulf killifish live in close association with the sediment and feed on benthic organisms that may be exposed to oil (Rozas and Lasalle 1990). Although many physiological effects have been reported for individual fish exposed to DHOS oil (Burggren et al. 2015; Dubansky et al. 2013; Whitehead et al. 2012), reports highlight a disconnect between individual and population level effects of oil spills (Able et al. 2015; Dubansky et al. 2014; Fodrie et al. 2014a). This conflicting information can be partially explained by the common belief that fish will avoid oil, although this is not likely the case with all species. It has been recently shown that Gulf killifish spent between 42 and 56% of their time in sediments containing weathered oil, showing no preference for unoiled sediments (Martin 2017). In that same study, Sheepshead minnow (*Cyprinodon variegatus*) and sailfin mollys (*Poecilia latipinna*) also showed no preference, spending between 42–62% and 44–56% of their time, respectively, over sediment containing weathered oil. Interestingly, the Gulf killifish avoided sediment containing fresh oil but still spent nearly 20% of the trial over the freshly oiled sediment (Martin 2017). This is likely sufficient to elicit a sustained physiological response to toxicants from the fresh oil. Behavioral tests in rock sole (*Pleuronectes bilineatus*) yellowfin sole (*P. asper*) and Pacific halibut (*Hippoglossus stenolepis*) also indicate that these fish species also do not always avoid oiled sediments but

prefer to associate with their ideal niche substrate regardless of the level of oiling (Moles et al. 1994). Such behavioral testing should be paired with physiological indices of individual exposure and effect to provide links that could ascent to describe and interpret population-level effects in future studies.

Oil derived from the diet has been shown to cause growth impairment in pink salmon, prolonging their time of vulnerability to larger predators, which was linked to population-level effects (Geiger et al. 1996, 1997; Sturdevant et al. 1996). These data also show evidence that some Gulf killifish in oiled sites were exposed to toxicants from oil through their diet. This underscores the need to monitor animal health across the manifold of biological function in order to best assess the long-term effects of crude oil exposure. These results illustrate the importance for assessment of multiple tissues to understand the integrated biological response to oil-derived toxicants. This is highlighted in the extrahepatic indications of AHR activity in situ, seen in the results presented. Although it is dogmatic to focus on the liver for such studies as this, extra-hepatic tissues contribute significantly to xenobiotic transformation prior to systemic transport of bioactive metabolites (James et al. 2001; Kleinow et al. 1998) and should be considered for future investigations.

Future studies should include multiple reference and affected sites to provide a more comprehensive overview when effects occur across a large geographic area, because it is important to note that there are not only differences in population responses to AHR ligands but differences in physiology between populations, which are likely to differentially affect the physiology and fitness of discrete populations (Oziolor et al. 2016; Whitehead et al. 2011). As such, further investigation of the effects of weathered oil in Barataria Bay sediments on the health of aquatic species is merited to monitor the rate of recovery in this region and the potential of ongoing exposure. Utilization of fine-scale physiological indices of health, such as immunological modulation, reproductive capacity, and physical performance, should be matched with genomic and genetic foundations to monitor the long-term effects of crude oil on resident species. Such data should include adequate number of sites and samples to provide sufficient statistical power to describe potential trends. Data would be best matched with more extensive forensic analytical chemistry of sediments and water to monitor site-specific changes that may present in heavily oiled locations where resident biota may be chronically exposed through the diet.

Supplementary Material

Refer to Web version on PubMed Central for supplementary material.

Acknowledgments

The authors thank Captain Anton Falcone for providing logistical support, field sampling expertise, and significant insight into planning multi-day sampling trips. They also thank Dr. Charlotte Bodinier for assistance processing microsomes and tissues for histology. Additional help in the field was provided under adverse conditions by Dr. Brooke Dubansky, Dr. Shujun Zhang, Steven Altomare, and Bradly Hoppe, and their help and sacrifice is appreciated.

Funding Sources This research was funded in part by the National Science Foundation (OCE-1314453 to F. G.), National Institute of Environmental Health Sciences (R01ES021934 to F. G.), National Institutes of Health (R15-ES016905-01 to C. D. R.) and Cossich, Sumich, Parsiola, and Taylor LLC, and the MDL 2179 Plaintiffs' Steering

Committee (to B. D. and F. G). Sponsors did not participate in the collection, analysis, or interpretation of data or the writing or editing of this manuscript.

References

Abel J, Haarmann-Stemmann T. An introduction to the molecular basics of aryl hydrocarbon receptor biology. Biol Chem. 2010; 391:1235–1248. [PubMed: 20868221]

Able KW, Lopez-Duarte PC, Fodrie FJ, Jensen OP, Martin CW, Roberts BJ, Valenti J, O'Connor K, Halbert SC. Fish assemblages in Louisiana salt marshes: effects of the Macondo oil spill. Estuaries Coasts. 2015; 38:1385–1398.

Atlas RM, Hazen TC. Oil biodegradation and bioremediation: a tale of the two worst spills in U.S. history. Environ Sci Technol. 2011; 45:6709–6715. [PubMed: 21699212]

Burggren WW, Dubansky B, Roberts A, Alloy M. Deepwater horizon oil spill as a case study for interdisciplinary cooperation within developmental biology, environmental sciences and physiology. World J Eng Technol. 2015; 3:7–23.

Carls MG, Holland LG, Short JW, Heintz RA, Rice SD. Monitoring polynuclear aromatic hydrocarbons in aqueous environments with passive low-density polyethylene membrane devices. Environ Toxicol Chem. 2004; 23:1416–1424. [PubMed: 15376527]

Carlson EA, Li Y, Zelikoff JT. Benzo a pyrene-induced immunotoxicity in Japanese medaka (*Oryzias latipes*): relationship between lymphoid CYP1A activity and humoral immune suppression. Toxicol Appl Pharmacol. 2004a; 201:40–52. [PubMed: 15519607]

Carlson EA, Li Y, Zelikoff JT. Suppressive effects of benzo[a]pyrene upon fish immune function: evolutionarily conserved cellular mechanisms of immunotoxicity. Mar Environ Res. 2004b; 58:731–734. [PubMed: 15178106]

Celander MC. Cocktail effects on biomarker responses in fish. Aquat Toxicol. 2011; 105:72–77. [PubMed: 22099347]

Crowe KM, Newton JC, Kaltenboeck B, Johnson C. Oxidative stress responses of Gulf killifish exposed to hydrocarbons from the Deepwater Horizon oil spill: potential implications for aquatic food resources. Environ Toxicol Chem. 2014; 33:370–374. [PubMed: 24122941]

Dubansky B, Whitehead A, Miller J, Rice CD, Galvez F. Multi-tissue molecular, genomic, and developmental effects of the Deepwater Horizon oil spill on resident Gulf killifish (*Fundulus grandis*). Environ Sci Technol. 2013; 47:5074–5082. [PubMed: 23659337]

Dubansky B, Whitehead A, Rice CD, Galvez F. Response to comment on "multi-tissue molecular, genomic, and developmental effects of the Deepwater Horizon oil spill on resident Gulf killifish (*Fundulus grandis*). Environ Sci Technol. 2014; 14(13):7679–7680.

Fodrie FJ, Able KW, Galvez F, Heck KL Jr, Jensen OP, Lopez-Duarte PC, Martin CW, Turner RE, Whitehead A. Integrating organismal and population responses of estuarine fishes in Macondo spill research. Bioscience. 2014a; 64:778–788.

Fodrie JF, et al. Integrating organismal and population responses of Gulf of Mexico fishes to the Macondo spill guides future research priorities. Bioscience. 2014b; 64(9):778–788.

Geiger H, Bue BG, Sharr S, Wertheimer AC, Willet TM. A life history approach to estimating damage to Prince William Sound pink salmon caused by the Exxon Valdez oil spill. Am Fish Soc Symp. 1996; 18:487–798.

Geiger HJ, Smoker WW, Zhivotovsky LA, Gharrett AJ. Variability of family size and marine survival in pink salmon (*Oncorhynchus gorbuscha*) has implications for conservation biology and human use. Can J Fish Aquat Sci. 1997; 54:2684–2690.

Hogan NS, Lee KS, Kollner B, van den Heuvel MR. The effects of the alkyl polycyclic aromatic hydrocarbon retene on rainbow trout (*Oncorhynchus mykiss*) immune response. Aquat Toxicol. 2010; 100:246–254. [PubMed: 20810174]

James MO, Tong Z, Rowland-Faux L, Venugopal CS, Kleinow KM. Intestinal bioavailability and biotransformation of 3-hydroxybenzo(a) pyrene in an isolated perfused preparation from channel catfish, *Ictalurus punctatus*. Drug Metab Dispos. 2001; 29:721–728. [PubMed: 11302939]

Kleinow KM, James MO, Tong Z, Venugopalan CS. Bioavailability and biotransformation of benzo[*a*]pyrene in an isolated perfused in situ catfish intestinal preparation. Environ Health Perspect. 1998; 106:155–166. [PubMed: 9449680]

Kokaly RF, Couvillion BR, Holloway JM, Roberts DA, Ustin SL, Peterson SH, Khanna S, Piazza SC. Spectroscopic remote sensing of the distribution and persistence of oil from the Deepwater Horizon spill in Barataria Bay marshes. Remote Sens Environ. 2013; 129:210–230.

Levine SL, Oris JT. CYP1A expression in liver and gill of rainbow trout following waterborne exposure: implications for biomarker determination. Aquat Toxicol. 1999; 46:279–287.

Lindsey S, Papoutsakis ET. The evolving role of the aryl hydrocarbon receptor (AHR) in the normophysiology of hematopoiesis. Stem Cell Rev Rep. 2012; 8:1223–1235.

Liu Z, Liu J, Zhu Q, Wu W. The weathering of oil after the Deepwater Horizon oil spill: insights from the chemical composition of the oil from the sea surface, salt marshes and sediments. Environ Res Lett. 2012; 7:14.

Martin CW. Avoidance of oil contaminated sediments by estuarine fishes. Mar Ecol Prog Ser. 2017 (in press).

McCormick SD. Endocrine control of osmoregulation in teleost fish. Am Zool. 2001; 41:781–794.

McNutt MK, Camilli R, Crone TJ, Guthrie GD, Hsieh PA, Ryerson TB, Savas O, Shaffer F. Review of flow rate estimates of the Deepwater Horizon oil spill. Proc Natl Acad Sci USA. 2012; 109:20260–20267. [PubMed: 22187459]

Mendelssohn IA, Andersen GL, Baltz DM, Caffey RH, Carman KR, Fleeger JW, Joye SB, Lin QX, Maltby E, Overton EB, Rozas LP. Oil impacts on coastal wetlands: implications for the Mississippi River Delta ecosystem after the Deepwater Horizon oil spill. Bioscience. 2012; 62:562–574.

Moles A, Rice S, Norcross BL. Non-avoidance of hydrocarbon laden sediments by juvenile flatfishes. Neth J Sea Res. 1994; 32:361–367.

Nakayama A, Riesen I, Kollner B, Eppler E, Segner H. Surface marker-defined head kidney granulocytes and B lymphocytes of rainbow trout express benzo a pyrene-inducible cytochrome P4501A protein. Toxicol Sci. 2008; 103:86–96. [PubMed: 18281257]

Nixon Z, Zengel S, Baker M, Steinhoff M, Fricano G, Rouhani S, Michel J. Shoreline oiling from the Deepwater Horizon oil spill. Mar Pollut Bull. 2016; 107:170–178. [PubMed: 27098990]

Oziolor EM, Dubansky B, Burggren WW, Matson CW. Cross-resistance in Gulf killifish (*Fundulus grandis*) populations resistant to dioxin-like compounds. Aquat Toxicol. 2016; 175:222–231. [PubMed: 27064400]

Pfaffl MW. A new mathematical model for relative quantification in real-time RT-PCR. Nucleic Acids Res. 2001; 29:2002–2007.

Pilcher W, Miles S, Tang S, Mayer G, Whitehead A. Genomic and genotoxic responses to controlled weathered-oil exposures confirm and extend field studies on impacts of the Deepwater Horizon oil spill on native killifish. PLoS ONE. 2014; 9:11.

Reinecke M, Segner H. Immunohistochemical localization of cytochrome P4501A in developing turbot, *Scophthalmus maximus*. Mar Environ Res. 1998; 46:487–491.

Reynaud S, Deschaux P. The effects of polycyclic aromatic hydrocarbons on the immune system of fish: a review. Aquat Toxicol. 2006; 77:229–238. [PubMed: 16380172]

Rice, CD. Fish immunotoxicology: understanding mechanisms of action. In: Schlenk, D., Benson, WH., editors. Target organ toxicity in marine and freshwater teleosts. Taylor and Francis Publishers; London: 2001. p. 96-138.

Rice CD, Schlenk D, Ainsworth J, Goksøyr A. Cross-reactivity of monoclonal antibodies against peptide 277–294 of rainbow trout CYP1A1 with hepatic CYP1A among fish. Mar Environ Res. 1998; 46:87–91.

Rozas LP, Lasalle MW. A comparison of the diets of Gulf killifish, *Fundulus grandis* Baird and Girard, entering and leaving a Mississippi brackish marsh. Estuaries. 1990; 13:332–336.

Sarasquete C, Segner H. Cytochrome P4501A (CYP1A) in teleostean fishes. A review of immunohistochemical studies. Sci Total Environ. 2000; 247:313–332. [PubMed: 10803558]

Silliman BR, van de Koppel J, McCoy MW, Diller J, Kasozi GN, Earl K, Adams PN, Zimmerman AR. Degradation and resilience in Louisiana salt marshes after the BP–Deepwater Horizon oil spill. Proc Natl Acad Sci. 2012; 109:11234–11239. [PubMed: 22733752]

Spies RB, Stegeman JJ, Hinton DE, Woodin B, Smolowitz R, Okihiro M, Shea D. Biomarkers of hydrocarbon exposure and sublethal effects in embiotocid fishes from a natural petroleum seep in the Santa Barbara Channel. Aquat Toxicol. 1996; 34:195–219.

Stevens EA, Mezrich JD, Bradfield CA. The aryl hydrocarbon receptor: a perspective on potential roles in the immune system. J Immunol. 2009; 127:299–311.

Sturdevant MV, Wertheimer AC, Lum JL. Diets of juvenile pink and chum salmon in oiled and non-oiled nearshore habitats in Prince William Sound, 1989 and 1990. Am Fish Soc Symp. 1996; 18:578–592.

Turner RE, Overton EB, Meyer BM, Miles MS, McClenachan G, Hooper-Bui L, Engel AS, Swenson EM, Lee JM, Milan CS, Gao H. Distribution and recovery trajectory of Macondo (Mississippi Canyon 252) oil in Louisiana coastal wetlands. Mar Pollut Bull. 2014; 87:57–67. [PubMed: 25176275]

Turner RE, McClenachan G, Tweel AW. Islands in the oil: quantifying salt marsh shoreline erosion after the Deepwater Horizon oiling. Mar Pollut Bull. 2016; 110:316–323. [PubMed: 27349381]

Tuvikene A. Resonses of fish to polycyclic aromatic-hydrocarbons (PAHs). Ann Zool Fenn. 1995; 32:295–309.

van der Oost R, Beyer J, Vermeulen NPE. Fish bioaccumulation and biomarkers in environmental risk assessment: a review. Environ Toxicol Pharmacol. 2003; 13:57–149. [PubMed: 21782649]

Van Veld PA, Stegeman JJ, Woodin BR, Patton JS, Lee RF. Induction of monooxygenase activity in the intestine of spot (*Leiostomus xanthurus*), a marine teleost, by dietary polycyclic aromatic hydrocarbons. Drug Metab Dispos Biol Fate Chem. 1988; 16:659–665. [PubMed: 2906586]

Van Veld PA, Westbrook DJ, Woodin BR, Hale RC, Smith CL, Huggett RJ, Stegeman JJ. Induced cytochrome P-450 in intestine and liver of spot (*Leiostomus xanthurus*) from a polycyclic aromatic hydrocarbon contaminated environment. Aquat Toxicol. 1990; 17:119–131.

Van Veld PA, Vogelbein WK, Cochran MK, Goksoyr A, Stegeman JJ. Route-specific cellular expression of cytochrome P4501A (CYP1A) in fish (*Fundulus heteroclitus*) following exposure to aqueous and dietary benzo[*a*] pyrene. Toxicol Appl Pharmacol. 1997; 142:348–359. [PubMed: 9070358]

Whitehead A, Roach JL, Zhang SJ, Galvez F. Genomic mechanisms of evolved physiological plasticity in killifish distributed along an environmental salinity gradient. Proc Natl Acad Sci USA. 2011; 108:6193–6198. [PubMed: 21444822]

Whitehead A, Dubansky B, Bodinier C, Garcia TI, Miles S, Pilley C, Raghunathan V, Roach JL, Walker N, Walter RB, Rice CD, Galvez F. Genomic and physiological footprint of the Deepwater Horizon oil spill on resident marsh fishes. Proc Natl Acad Sci. 2012; 109:20298–20302. [PubMed: 21949382]

Woodin BR, Smolowitz RM, Stegeman JJ. Induction of cytochrome P4501A in the intertidal fish *Anoplarchus purpurescens* by Prudhoe Bay crude oil and environmental induction in fish from Prince William Sound. Environ Sci Technol. 1997; 31:1198–1205.

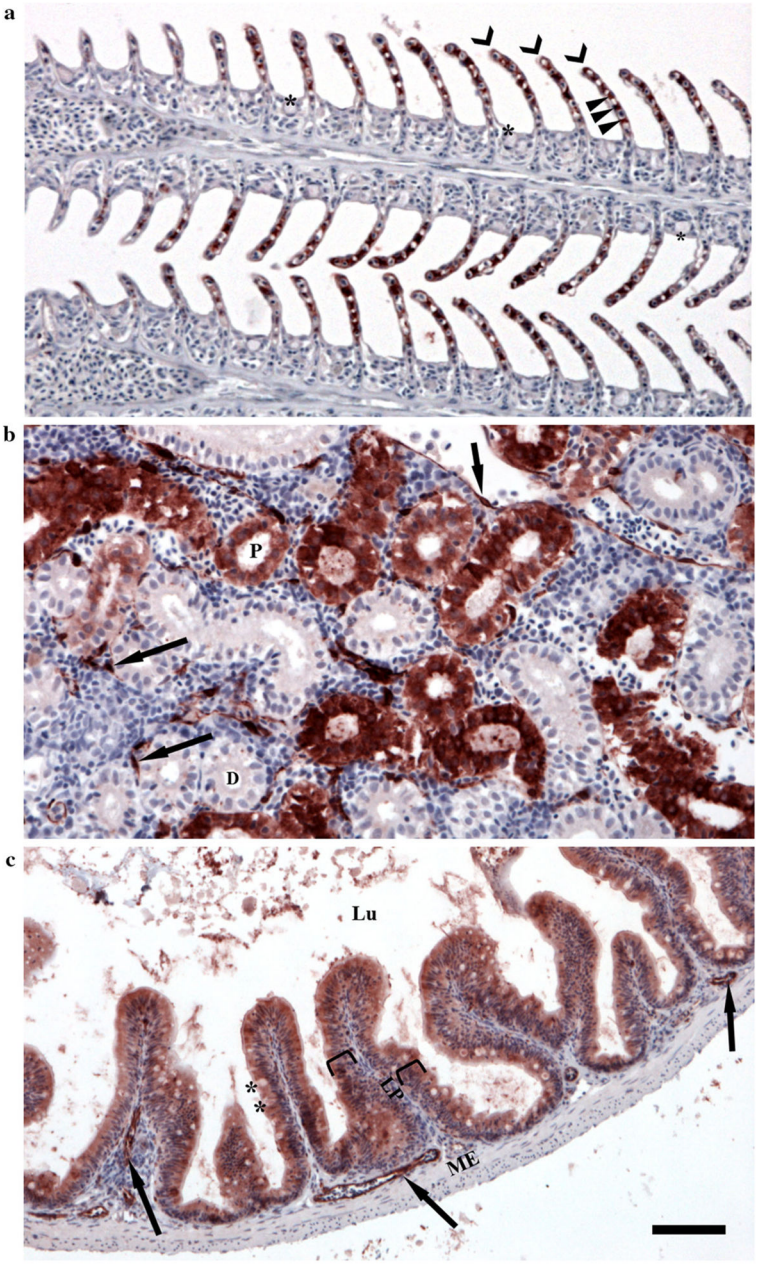

Fig. 1.

Scoring system for determining localization and abundance of CYP1A protein (*red* staining) in gills, head kidney, and intestine from adult Gulf killifish (*Fundulus grandis*). **a** Gills were scored according to degree of staining in pillar cells (*arrow heads*) along the lamellae (chevrons), and for the combined degree of staining in other remaining cells including mucus cells within the interlamellar region (*asterisks*), vascular endothelial cells (not identified in **a**, see **b** and **c** for examples of vascular endothelial cells), and epithelial cells covering the surface of the gill and the interlamellar region. **b** Head kidneys were scored for the staining of the epithelial cells of the distal and proximal tubules (D and P) and for the degree of staining in vascular endothelial cells (*arrows*). **c** Intestinal tissues were scored

based on degree of staining in the epithelial and mucus cells (*asterisks*) of the mucosal layer (*brackets*) and for the degree of staining of vascular endothelial cells. *Lu* lumen, *LP* lamina propria, *ME* muscularis externa. See Table 3 for additional information. All tissues sectioned at 4 μm and imaged with a 20X objective. Scale bar = 50 μm. All slides were counterstained with hematoxylin (*blue*)

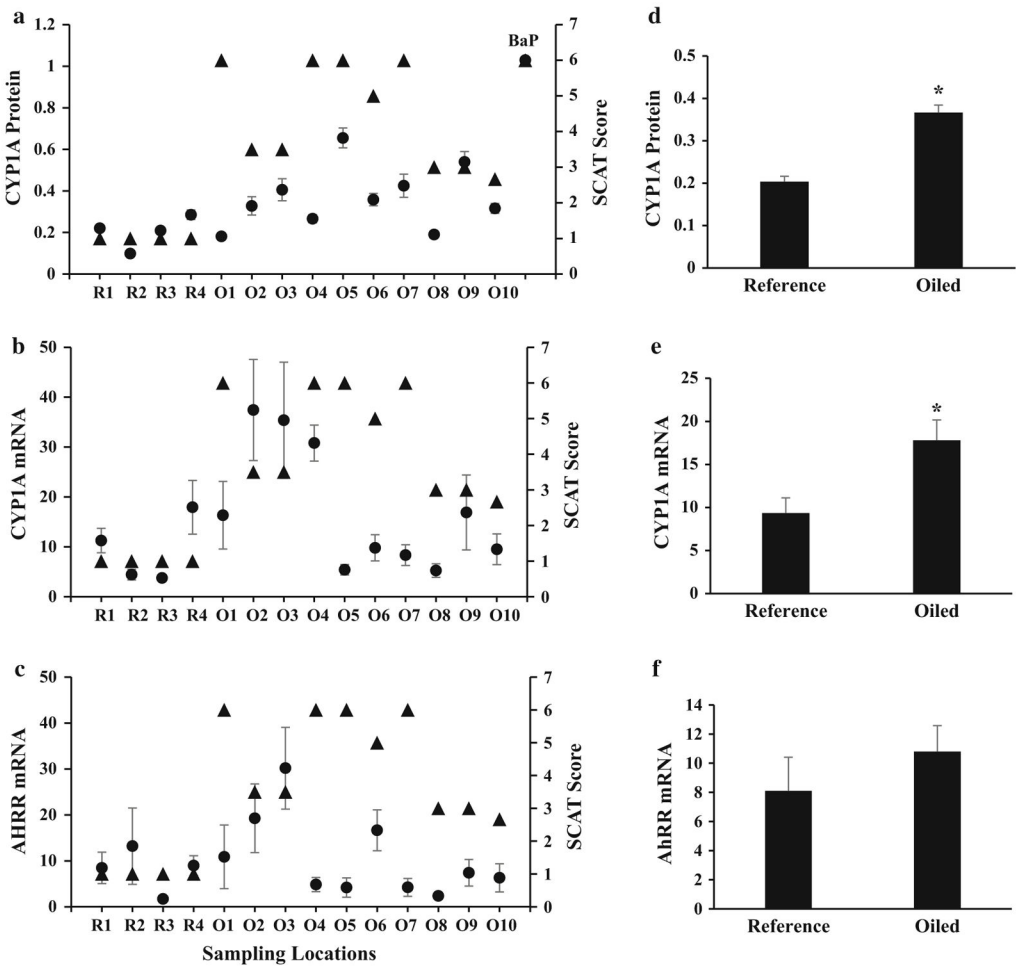

Fig. 2.

CYP1A protein, and CYP1A and AHRR mRNA transcript abundance in livers from fish collected from oiled (O1–O10) and reference sites (R1–R4) in the Barataria Basin. **a** Relative concentration of CYP1A protein (*circles*) using ELISA for mAb C10-7 ($N = 12$) and SCAT visible data (*triangles*) at time of sampling. **b** Fold change of liver CYP1A mRNA (*circles*) ($N = 7–8$) and SCAT visible data (*triangles*) at time of sampling. **c** Fold change of liver AHRR mRNA (*circles*) ($N = 7–8$) and SCAT visible data (*triangles*) at time of sampling. **d** Mean CYP1A protein, **e** mean CYP1A mRNA, and **f** mean AHRR mRNA values from all oiled sites versus all reference sites ($N = 50–52$). *Asterisks* indicate $P < 0.05$, *t* test. *Error bars* indicate standard error of the mean. See text for further details

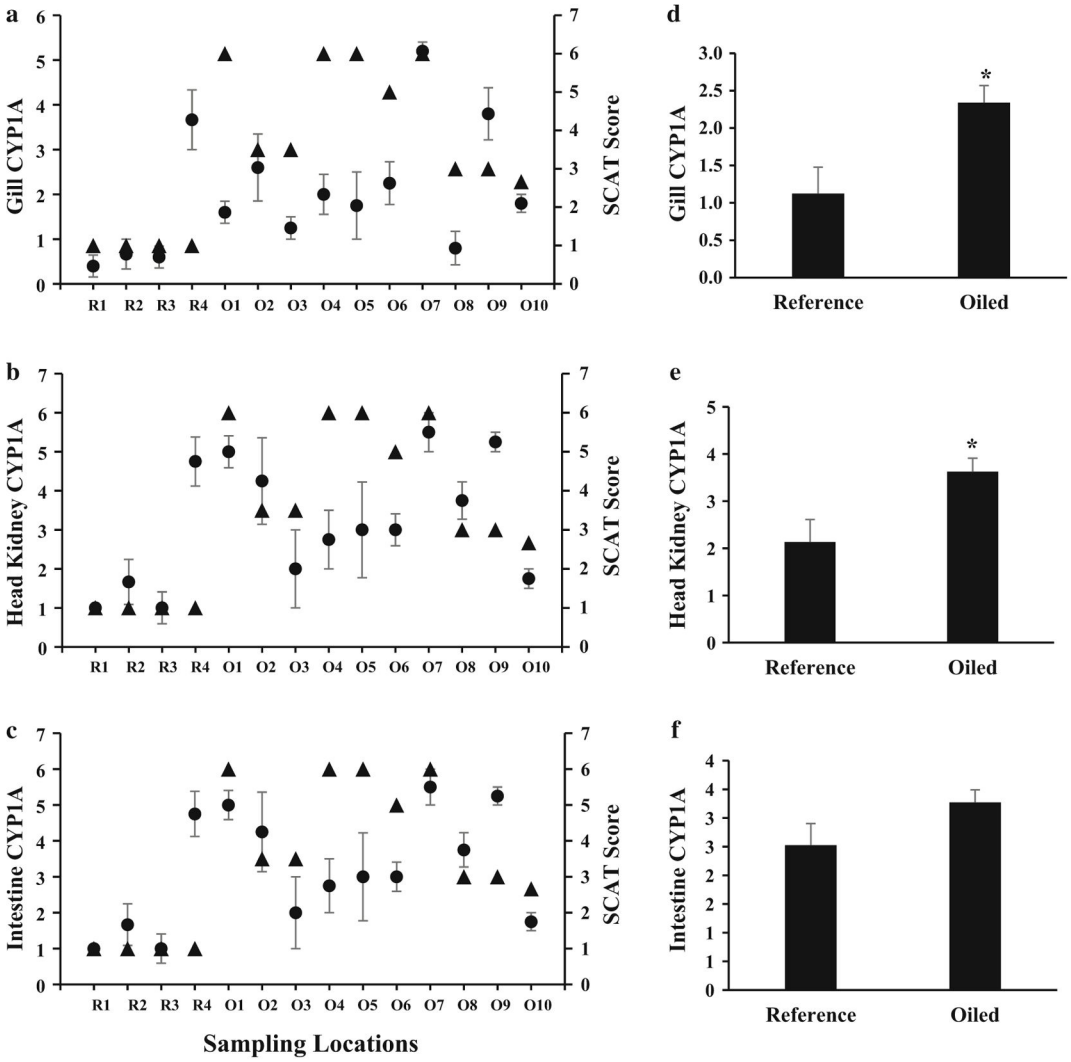

Fig. 3.

CYP1A immunostaining intensity scores for gill, head kidney, and intestinal tissues collected from oiled (O1–O10) and reference sites (R1–R4) in the Barataria Basin. **a** Average CYP1A intensity scores for gill ($N = 3–5$) compared with SCAT visible oiling score (*triangles*) at time of sampling. **b** Average CYP1A intensity scores for head kidney ($N = 3–4$) compared with SCAT visible oiling score (*triangles*) at time of sampling. **c** Average CYP1A intensity scores for intestine ($N = 4–5$) compared with SCAT visible oiling scores (*triangles*) at time of sampling. Displays average CYP1A intensity scores for **d** gill ($N = 16–47$), **e** intestine ($N = 15–40$), and **f** head kidney tissues ($N = 19–48$) from all oiled sites versus all reference sites. *Error bars* indicate standard error of the mean. *Asterisks* indicate $P < 0.05$, *t* test. See text for further details

Table 1

Sample sites, including the internal identification (Site I.D.) of each location, location name, global-positioning system coordinates, sampling date, and average of SCAT data within 100 m of each site as a measure of site oiling at the site of fish collection

I.D.	Location description	Latitude	Longitude	Sampling date	Maximum SCAT observations	Average SCAT value*
R1	Southwest Wilkinson Bay	29.463360°	−89.932190°	11/8/2010	No oil observed	1
R2	West Wilkinson Bay	29.475360°	−89.933780°	11/8/2010	No oil observed	1
R3	Southeast Mud Lake	29.460794°	−89.981086°	12/30/2010	No oil observed	1
R4	Northwest Bay Sansbois	29.474961°	−89.779056°	12/30/2010	No oil observed	1
O1	South Wilkinson Bay	29.458204°	−89.909429°	11/11/2010	Heavy	6
O2	Southeast Bay Jimmy	29.445140°	−89.880103°	10/30/2010	Heavy	3.5
O3	Northwest Bay Batiste	29.479324°	−89.863246°	10/30/2010	Heavy	3.5
O4	Bayou Dulac	29.455440°	−89.805176°	10/30/2010	Heavy	6
O5	South Wilkinson Bay	29.464950°	−89.911604°	11/10/2010	Heavy	6
O6	Barataria Bay	29.436544°	−89.884232°	11/10/2010	Heavy	5
O7	Saint Mary's Point	29.447048°	−89.937137°	11/11/2010	Heavy	6
O8	Eastern Barataria Bay	29.424640°	−89.825160°	11/8/2010	Moderate	3
O9	Northeast Bay Batiste	29.461580°	−89.817460°	11/8/2010	Moderate	3
O10	Eastern Barataria Bay	29.432760°	−89.828100°	11/11/2010	Light	2.66

*Collective SCAT oiling observations within 100 m of sites. See SCAT value descriptions at http://gomex.erma.noaa.gov

Table 2

Primer sequences and RT-PCR operation data

Gene name	Accession #	Primer sequence (5′ → 3′)	T_m °C	Product size (bp)
AHRR	AF443441.1	F: TTG TCT CGA AGC TGT ATG GCT CGT R: ATC TTA ATG GGC GGC ATT TCA GGC	57	124
CYP1A	AF026800.1	F: AAG CAA GAG GGA GAG AAG GTC CTT R: TGT GCT TCA TCG TGA GGC CAT ACT	57	150
18S	M91180.1	F: TTC GTA TTG TGC CGC TAG AGG TGA R: TTC GAA CCT CCG ACT TTC GCT CTT	57	125

Table 3

Description of criteria used for determining degree of immunoreactivity for CYP1A protein in gill, head kidney, and intestine, based on categories of major sites of CYP1A protein expression and relative staining

Tissue	Category	Description	Relative staining	Score
Gill	1	Gill pillar cells	No staining observed	0
			Some pillar cells stained	1
			Most pillar cells stained with some saturated	2
			Pillar cells saturated with stain	3
	2	Other gill cells (epithelial cells, mucus cells, vascular endothelial cells)	No staining observed	0
			Light pink	1
			Observation of moderate staining of some non-pillar cells	2
			Pervasive staining of epithelial cells, mucus cells	3
Head kidney	1	Tubules	No staining—light pink	0
			Light pink—red	1
			Red with some tubules saturated dark red	2
			Majority of tubules saturated red	3
	2	Vascular endothelial cells	No staining	0
			Light pink	1
			Red	2
			Majority of VECs saturated dark red	3
Intestine	1	Mucosal layer	No staining—light pink	0
			Some staining of mucosal layer	1
			Consistent, light staining in mucosal layer	2
			Majority of mucosal layer saturated red	3
	2	Vascular endothelial cells	No vascular endothelial cells stained	0
			Slight staining of some vascular endothelial cells	1
			Moderate staining of vascular endothelial cells	2
			Heavy staining in vascular endothelial cells	3

Table 4

Degree of oiling at each field site based on SCAT classification at time of sampling

SCAT classification→	No oil observed	Tar balls	Very light	Light	Moderate	Heavy	
SCAT color numerical value→	1	2	3	4	5	6	
Site ID							SCAT average
R1	+						1
R2	+						1
R3	+						1
R4	+						1
O1						+	6
O2	+					+	3.5
O3	+		+	+		+	3.5
O4						+	6
O5						+	6
O6				+	+	+	5
O7						+	6
O8	+				+		3
O9	+				+		3
O10	+		+	+			2.7

Each SCAT classification designated at sampling locations is indicated with + symbol. Sites with multiple + values indicate the multiple SCAT designations observed within 100 m of a sampling location. SCAT designations were averaged for each site